

Real time monitoring of screw insertion using acoustic emission can predict screw stripping in human cancellous bone.

Wright BJ^{1,2,3}, Grigg S⁴, Bergsaker AS⁵, Brattgjerd JE^{2,3}, Steen H³, Pullin R⁴

1. Vestre Viken, Ringerike Sykehus, Hønefoss, Norway
2. Institute for Clinical Medicine, University of Oslo, Norway
3. Biomechanics Laboratory, Orthopaedic Division, Oslo University Hospital, Norway
4. Cardiff School of Engineering, Cardiff University, Cardiff, UK
5. IT for Research, University Center for IT, University of Oslo, Norway

Corresponding author: Bryan Joseph Wright email: bjwright3@yahoo.com

Permanent address: Hartmanns Vei 31b, 0284 Oslo, Norway

Word count article = 3520

Word count abstract = 250

Abstract

Background: To develop experience, orthopedic surgeons train their own proprioception to detect torque during screw insertion. This experience is acquired over time and when implanting conventional/non-locked screws in osteopenic cancellous bone the experienced surgeon still strips between 38-45%. Technology needs to be investigated to reduce stripping rates. Acoustic-Emission technology has the ability to detect stress wave energy transmitted through a screw during insertion into synthetic bone. Our hypothesis is Acoustic-Emission waves can be detected through standard orthopedic screwdrivers while advancing screws through purchase and overtightening in cancellous human bone with different bone mineral densities replicating the clinical state.

Methods: 77 non-locking 4mm and 6.5mm diameter cancellous bone screws were inserted through to stripping into the lateral condylar area of 6 pairs of embalmed distal femurs. Specimens had varying degrees of bone mineral density determined by quantitative CT. Acoustic-Emission energy and axial force were detected for each test.

Results: The tests showed a significant high correlation between bone mineral density and Acoustic-Emission energy with $R=0.74$. A linear regression model with the mean stripping load as the dependent variable and mean Acoustic-Emission energy, bone mineral densities and screw size as the independent variables resulted in $r^2=0.94$.

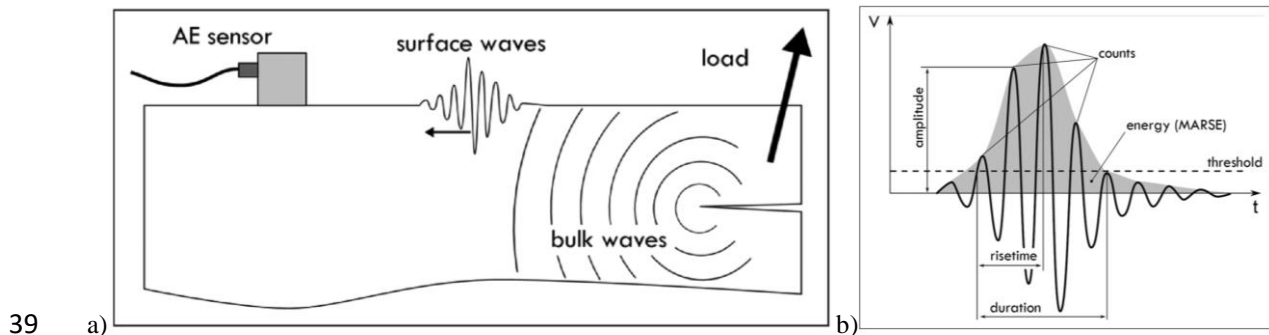
Interpretation: This experiment succeeded in testing real time Acoustic-Emission monitoring of screw purchase and overtightening in human bone. Acoustic-Emission energy and axial compressive force have positive high correlation to bone mineral density. The purpose is to develop a known technology and apply it to improve the bone-metal construct strength by reducing human error of screw overtightening.

1 **1. Introduction**

2
3 In orthopaedic surgery the screw, simply explained a device that converts torque into compressive
4 force, is widely employed in nearly all constructs used for fracture fixation. A screw under load
5 creates tension within the screw and compression between the threads and the head. The ability for
6 any screw to transform the torque applied into tension in the screw and compression between the
7 threads and the screw head is dependent on the material that screw is purchased in. When fixing
8 fractures in osteopenic or osteoporotic cancellous bone, screw purchase and its ability to apply
9 compressive force without destroying the purchase material (stripping) is completely dependent on
10 the surgeon's own experience [Maguire1995]. In order to develop experience, orthopaedic surgeons
11 train their own proprioception to detect both the appropriate torque and the compressive force being
12 applied to the screw during insertion. This experience is acquired over time with a learning curve and
13 can be at the expense of construct stability. When implanting screws in cancellous bone the
14 experienced surgeon is still far from perfect. In a study testing the need for bone filler in augmenting
15 of screw fixation, a group of experienced trauma surgeons inserted 225 screws into 37 ankle fracture
16 patients over the age of 50. Of these 225 screws, 86 screws (38%) stripped during the procedures
17 [Andreassen2004]. This was further examined by Stoesz et al when they tested 10 orthopaedic
18 surgeons in the tightening of 240 screws in synthetic bone and 109 (45.4%) were stripped. During the
19 stripping process 90% of the time the surgeon did not notice that the screw was stripped [Stoesz2014].
20 When a screw is stripped, the pull-out strength of that screw decreases by 80% [Collinge2006]
21 consequently decreasing the overall construct strength. This can lead to construct failure with
22 increased morbidity to the patient. Torque monitoring has not been an ideal method in detecting
23 screw purchase particularly because of the wide variation of bone mineral density in the older patient
24 population [Tsuji2013]. In addition, Tsuji et al. showed that the stopping torque is similar to the
25 stripping torque, which gives screw purchase a 'plateau' characteristic. Torque resistance stops
26 increasing, requiring the surgeon to decide when to stop turning based on the torque response. In
27 fragile bone this difference in torque response is difficult to feel and even in experienced hands
28 overtightening occurs too often.

29 Alternative detection technology needs to be investigated. Acoustic Emission (AE) monitoring is a
30 well-established Non-Destructive Testing (NDT) technique. Energy is released when deformation
31 and damage grow within a material, this energy propagates as ultrasonic waves and is detectable using
32 piezoelectric transducers (Figure 1). This technology, because of advances in computing, has been
33 studied at an increased frequency in orthopaedic surgery. The reason is that AE monitoring has the
34 ability to detect crack formation in bone at such an early point that a catastrophic material failure can
35 be avoided [Kapur2016, Rashid2012]. A screw stripping in bone during fracture surgery is a type of

36 catastrophic material failure. In a previous study from this group, it was shown that AE waves were
37 readily detected in synthetic bone during screw purchase, and a pattern was detected prior to screw
38 stripping [Pullin2017; Fig 1].



40 Figure 1: a) Working principle of AE, a crack is formed in the material generating energy waves that are detected on the
41 surface by the AE sensor. b) Typical parameters for an AE event [pullin2017]

42

43 The aim of the current study is to detect AE waves in previously validated formalin fixed cadaver
44 femurs [Wright2018]. There is currently no commonly used method to assist surgeons in the
45 prevention of non-locking cancellous screw overtightening other than the surgeons own experience.
46 As shown above there is a large amount of surgeon related error. New technology, like AE
47 monitoring, needs to be investigated to help reduce the rate of stripping. The surface waves that are
48 detected can indicate non-destructive micro-cracking that can be a warning before catastrophic
49 material failure or screw stripping. The ultimate aim is to gain further ground in the development of a
50 real-time AE monitoring system, capable of detecting screw purchase and decrease the occurrence of
51 overtightening. The hypothesis is that AE waves can be detected through a standard orthopaedic
52 screwdriver while advancing screws through purchase and into overtightening in cancellous human
53 bone. The secondary hypothesis is that there is a positive relationship between the AE energy
54 captured through the screws and the bone mineral density of the distal femurs. This will help validate
55 the technique by showing that detected AE energy waves are able to delineate and differentiate
56 between varying degrees of osteopenic bone.

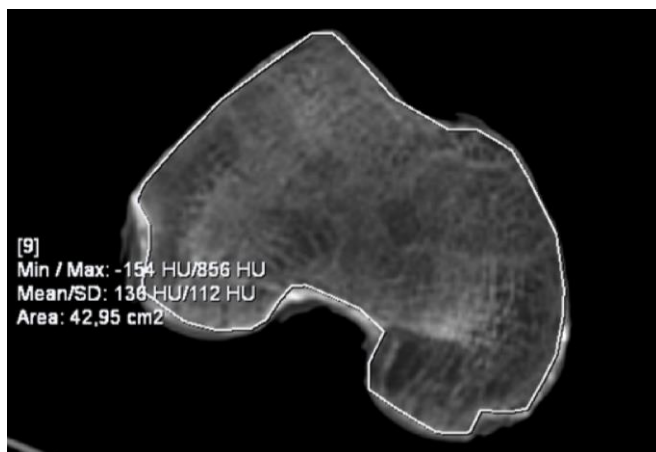
57

58 2. Methods

59

60 Two different sets of tests were performed on the lateral condyles of distal human femurs. Six pairs
61 of whole femurs without visible, radiological or historically significant bone pathology were
62 harvested from human cadavers donated for post mortem research purposes at the Division of
63 Anatomy, University of Oslo, Norway. Four pairs of female femurs and two pairs of male femurs

64 were used. The six pairs had a mean age of 82 (68–89) years. Each cadaver had been prepared in
65 5.6% formalin embalming solution and preserved in 40% ethanol according to a standardized routine
66 procedure. Quantitative computed tomography (QCT) was used to assess bone mineral parameters as
67 calcium density and calcium mass for all femurs in a Siemens SOMATOM Definition Edge (Siemens
68 Healthcare GmbH, Erlangen, Germany) with parameters for a bone scan (100 mA, 120 kV, 1mm
69 slice). Bone mineral content measurements were made in cross sectional slices perpendicular to the
70 longitudinal axis in the metaphyseal center level of the condyles. Syngo.via imaging software
71 (Siemens Healthcare GmbH, Erlangen, Germany) was used to draw a region of interest (ROI) around
72 the condylar cross-sectional area (Figure 2). The ROI included the axial slice orientated to include
73 both condyles proximal to the trochlear groove. The ROI also excluded the thin cortical wall in order
74 to measure a more accurate density calculation of the predominantly cancellous bone. The bone
75 mineral parameters that were used are QCT density and mass. Density was thus expressed as the mean
76 number of Hounsfield Units (HU) within the ROI. Bone mass was calculated as the mathematical
77 product of density and area cm^2 within the ROI and reflected radiological mineral mass
78 [Lagravère2006]. The tests were performed on the lateral condyles because they contain cancellous
79 bone that is the most osteopenic in nature compared to the rest of the femur.

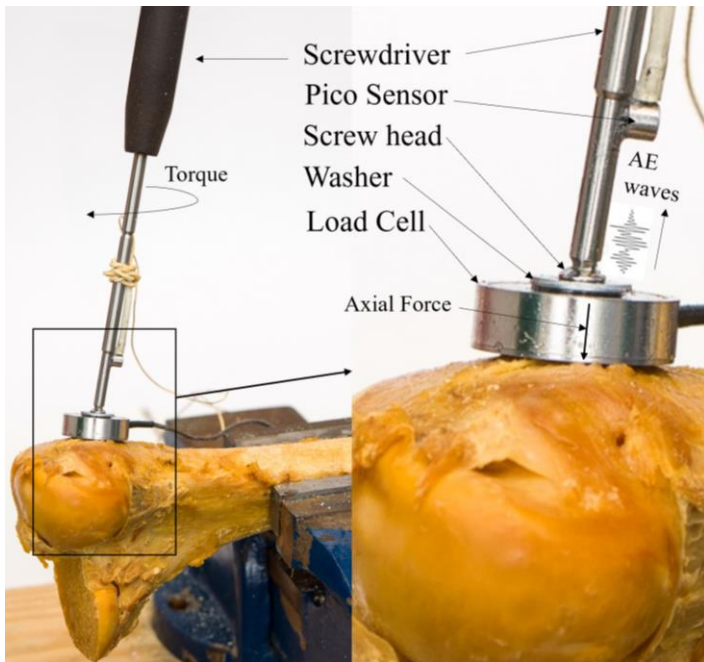


80
81 Figure 2: CT image of a cross sectional intercondylar axial slice of a left distal femur with the ROI drawn around excluding
82 the thin cortical wall.

83 AE data was collected using a National Instruments PXIe-1071 (National Instruments, Austin,
84 TX,USA), this instrument is designed for receiving input from a broad spectrum of measurements and
85 test applications, and combining them in a specifically designed Laboratory Virtual Instrument
86 Engineering Workbench (LabVIEW) (National Instruments, Austin, TX,USA). The data acquisition
87 environment LabVIEW allows for the creation and combining of the different user interfaces for each
88 measurement. AE waveforms generated by the screw to bone surface contact and cutting were
89 converted to electrical signals using a Mistras Pico piezoelectric sensor (200-750 KHz lightweight
90 mini, Physical Acoustics, NJ, USA) bonded with superglue to the screwdriver, as shown in Figure 3.

91 The signal was amplified using a Mistras 2/4/6 preamplifier with built in 20kHz to 1,200kHz
92 analogue filter and external power source. Data was collected at a sample rate of 2MHz with 2ms
93 worth of data being collected per hit and a timeout period of 3ms. A threshold of 0.1V (60dB) was
94 used to trigger the recording of data, with a 400µs pre-trigger. As well as AE, the system collected the
95 axial load through the screw using a doughnut load cell (LCMWD-1KN, OMEGA Engineering, Inc.
96 CT, USA) which was positioned between the bone and the head of the screw seen in Figure 3. The
97 load cell captures the axial force being applied by the user during turning and, because of its position,
98 it also measures the axial force being generated between the screw head and the screw threads during
99 and after each turn. When the screw begins to tighten the axial force generated by the screw threads
100 does not dissipate between turns, because the material is holding it in a compressive force between the
101 screw head and the load cell. When the axial force fails to increase during a turn, the material the
102 screw was purchased in has failed. In the screw purchase process there has been shown to be an
103 increase in axial force together with strain from torque and AE energy [pullin2017]. In the synthetic
104 bone model, even with continued screwing past the point of stripping, the axial force dramatically
105 decreased together with the strain caused by torque and AE energy. This gave a reliable subjective
106 method for determining real-time stripping that could be correlated with our AE data. The advantage
107 of the LabVIEW system, and the reason it was chosen, over a traditional AE system is its versatility.
108 It is able to collect and analyse multiple data sources like the AE signals and force together with time
109 and be used to produce multiple output options.

110

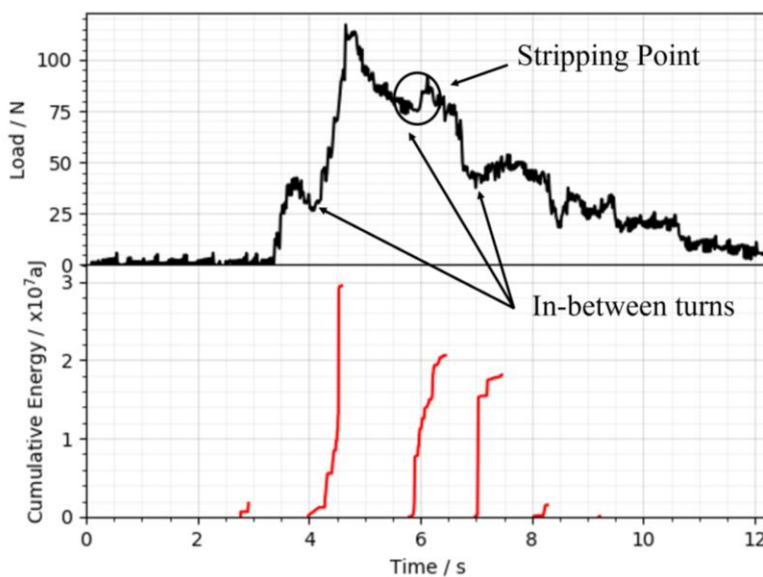


111

112 Figure 3 – Screwdriver delivers torque to the screw which creates an axial load captured by the load cell. The
113 screwthread/bone interface also is producing AE waves that travel through the screw and the screwdriver, and are then
114 captured by the PICO sensor bonded to the screwdriver.

115

116 Once collected, data was post processed using Python programming language. This involved
117 extracting several parameters including amplitude, duration and absolute energy from each AE event
118 (see Figure 1). The AE data can then be automatically split into data-pre-turn by finding the points
119 where no AE data is seen for 0.2s, which indicates that the screwdriver is not turning. The data was
120 then plotted in terms of load and cumulative energy per turn vs time, an example of which is shown in
121 Figure 4. The load in Figure 4 (continuous line) is seen to drop in-between turns, this is a result of the
122 force being applied by the screwdriver being removed, as well as some relaxation of the screw. As a
123 result of this the point of stripping is not necessarily the point of maximum load, but instead the point
124 where the load drops whilst AE data is being recorded (red line). In many cases this was the
125 maximum load, however in others, such as Figure 4 where the stripping point has been labelled, it was
126 not. When the point of stripping is identified the total AE energy produced prior to stripping can then
127 be found.



128

129 Figure 4 – Load vs Time over, and the same test Cumulative AE energy per turn vs Time under (Test 18_5) (see txt)

130 The first set of tests were performed on all of the right femurs at the lateral epicondyle. A standard
131 large fragment set (Depuy Synthes Johnson & Johnson Medical West Chester, PA, USA) was used.
132 Each hole was pre-drilled with a 3.2mm diameter drill bit and a 30mm long 6.5mm diameter partially
133 threaded cancellous bone screw was inserted. The second set of tests were done on all of the left
134 femurs at the lateral epicondyle. A standard small fragment set (Depuy Synthes Johnson & Johnson
135 Medical West Chester, PA, USA) was used. Each hole was pre-drilled with a 2.5mm diameter drill

136 bit and a 30mm long 4.0mm diameter partially threaded cancellous bone screw was inserted, both
137 tests as per manufacturer's instructions. Each cancellous screw from both the large and small
138 fragment set was inserted, gained purchase and proceeded to stripping. 5 to 9 tests were performed on
139 each femur in order to capture adequate AE signals. As seen in Figure 2 the trabecular architecture is
140 heterogeneous and not uniform, so more samples were taken when a larger range of axial forces were
141 obtained during tests.

142 2.1 Statistics

143 Spearman correlation was used as well as a linear regression model with robust standard errors (due to
144 small sample size). Both were run in SPSS statistical software (IBM Corporation, New York, USA).
145 The magnitude of the correlation coefficients were interpreted according to the rule of thumb by
146 Hinkle (negligible: 0.00–0.30; low: 0.30–0.50; moderate: 0.50–0.70; high: 0.70–0.90 and very high:
147 0.90–1.00) [Hinkle2003].

148

149 3. Results

150

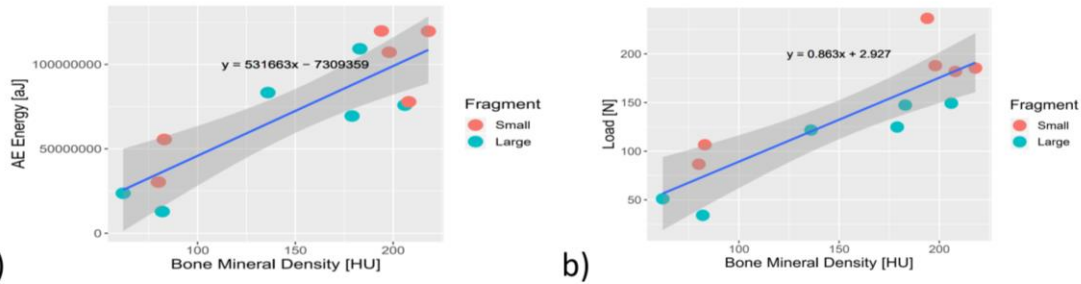
151 A total of 77 test were completed, 41 on the six right femurs and 36 on the six left femurs. In each
152 test the screw was tightened at a normal rate a doctor uses in the operating room by an experienced
153 orthopaedic trauma surgeon and then continued through to stripping. Stripping was shown when the
154 axial load began to decrease, because the bone material has failed and can no longer hold the
155 compressive axial force between the screw head and the loadcell. The mean cumulative AE energy
156 and mean stripping load for each bone were correlated to each other and to the bone mineral density.
157 Each of the tests showed a high correlation coefficient and all were significant (See Table 1).

158 Table 1. Results of the Spearman correlation (R). BMD – Bone Mineral Density, AE – Acoustic Emission

Test	R	Significance
BMD v Stripping Load	0.867	p < 0.01
BMD v AE Energy	0.741	p < 0.01
AE Energy v Stripping Load	0.888	p < 0.01

159

160 A linear correlation was seen for the bone mineral densities and the mean AE energy and load, as
161 shown in the figure 5 graphs.



162

163 Figure 5 – Bone mineral density plotted against acoustic emission energy (a) and against load (b). The different fragment
 164 sizes are indicated with either a red (small) or green (large) dot. The corresponding linear model is included in the plot (blue
 165 line), with the dark grey representing the 95% confidential interval. Graph produced using R (R Core Team, 2019) and
 166 ggplot2 [wickham2016].

167 A linear regression model was investigated with the mean stripping load as the dependent variable and
 168 mean AE energy, bone mineral densities and fragment size as the independent variables. The
 169 parameters from the regression model using small fragment as an example, with corresponding
 170 significance levels are presented in Table 2. The AE energy mean value has been rescaled by a factor
 171 of 1 million, equivalent to giving the measurements in pico-J instead of atto-J. This was done to
 172 improve interpretability of the model. All variables have a significant effect on the measured stripping
 173 load. An increase in bone mineral density of 1 HU is expected to increase load by 0.385 N, provided
 174 all other variables are kept constant. Similarly, an increase in AE energy of 1 pJ is expected to
 175 increase load by 0.794 N. All of these results are in keeping with the correlation analysis indicating
 176 that there is a positive linear relationship between both load and BMD, as well as load and AE energy.
 177 Interaction effects of mean AE energy, mean BMD and fragment size were also examined, but none
 178 of these were found to have a significant effect on the model.

179 Table 2. Parameters from the linear regression model with robust standard errors. The model consisted of the stripping load
 180 as the dependent variable and AE energy, bone mineral density and fragment size as the independent variables. B is the
 181 unstandardized correlation coefficient and the rate of change per unit. a - Parameter omitted due to redundance, as it is the
 182 reference category for the fragment size variable.

Parameter	B	95% Confidence interval		p-value
		Lower	Upper	
Small Fragment [N]	32.895	21.512	44.278	<0.001
Large Fragment	0 ^a			
BMD [HU]	0.385	0.212	0.558	<0.001
AE Energy [pJ]	0.794	0.386	1.203	<0.001

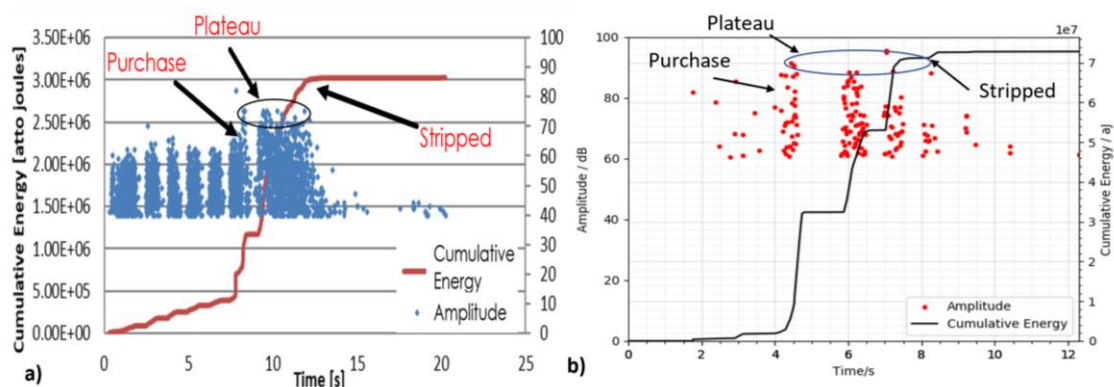
183

184 **4. Discussion**

185

186 In both the small and the large fragment screw group a clear positive high correlation was found
187 between the stripping load, the bone mineral density and the AE energy. Screw threads that are
188 overtightened or stripped cause a considerable amount of damage in bone, this was visibly shown in
189 the previous study done by this group with synthetic bone [pullin2017]. The compressive and
190 stripping force applied to the screw causes shear and crushing, affecting the area of trabecula around
191 the screw threads. This overall bone breaking process releases high rate AE energy that was detected.
192 Figure 5 shows that the bone mineral density is the material property that is directly correlated to the
193 amount of AE energy captured and the amount of compressive force a screw is able to produce. This
194 makes sense because the higher density means a larger amount of trabecular bone around the screw
195 threads. This in turn translates to increased amounts of organic and mineral material components of
196 bone being damaged between the threads. The damage of the material components of bone is
197 essentially their covalent bonds which normally hold them together being broken, releasing energy,
198 and hence an increase in AE energy. A denser trabecular environment also increases the resistance to
199 failure, hence a higher load. Similar to previous synthetic bone tests, each test in the cancellous bone
200 had an energy peak and brief plateau before a subsequent decrease (Figure 6). This is likened to the
201 stopping and stripping torque. The stopping torque is the ideal torque applied to a screw thought to
202 give the best construct stability. The stopping torque has been shown to be anywhere between 66%
203 and 86% of the maximum or stripping torque [aziz2014]. In Figure 6 the plateau area of the AE
204 energy signals (the blue dots and red dots) is the area where we find the stopping torque. Tankart et al
205 found that there is no significant difference in the pull-out strength of a screw after it is tightened to
206 just 50% of the stripping torque [tankart2013].

207



208 Figure 6 – Example of acoustic emission output of screw stripping showing the point of purchase, plateau and stripping. a)
209 synthetic bone b) current cadaver bone.

210 The ranges of resistance generated at the stopping torque during screw purchase is the elastic energy
211 accumulated from the trabecular bone before the shearing and crushing of permanent deformation.
212 This elastic energy as well as the shearing and crushing are all producing AE signals. This is seen in
213 both graphs in figure 6, after screw purchase the cumulative AE energy slope is almost vertical with
214 each turn of the screwdriver, with a slight change in slope and then flatline. In this there can be a
215 possible indicator of impending stripping. In the literature this is further confirmed by microCT
216 imagery where it has been shown that there is little to no damage seen in the microarchitecture of
217 trabecula when a screw is inserted up to 80% of the stripping torque [ryan2016].

218 The bone mineral density used is the mean number of Hounsfield Units (HU) found on the axial slice
219 of the mid-condylar area of each distal femur. This is a heterogeneous area of cancellous bone which
220 gives a range of stripping loads and AE signals. Because the bone mineral density was a mean, it was
221 decided to use the means for the stripping load and the means for the AE energy to compare like with
222 like. Embalmed bone was used instead of fresh frozen bone and some might argue that this is a
223 limitation to the study. A previous study from this group [Wright2018] showed that the bone mineral
224 parameters and the biomechanical properties of embalmed bone continue to correlate and that the
225 literature has not shown a clear difference between fresh frozen and embalmed bone during
226 biomechanical testing. A limitation to the study is the possible error of choosing the stripping load,
227 because of the axial force introduced through the screwdriver by the user. In addition to the load cell,
228 a strain gauge could have been mounted to the screwdriver to also calculate a value for torque which
229 in turn could have given a more accurate stripping endpoint. This is a limitation to the study. The
230 justification for not using a strain gauge was that the previous study done by this group [pullin2017]
231 showed that AE signal mirrors torque and that the logistics of including one in the experimental set up
232 was not possible at the time.

233 Standard training methods are taught to trainee surgeons on how tight screws should be. The two
234 finger tightness method is used the most. The two finger method is very vague and shown to be
235 inadequate and inaccurate [acker2016]. When surgeons were shown a digital and graphical
236 visualization of real time torque of screws being purchased into standardized osteoporotic synthetic
237 bone, the incidence of stripping decreased from 40% to 15% [gustafson2016]. Torque metres and
238 torque limited motorized drills and screwdrivers have had some success in the laboratory. They are
239 dependent on knowing or calculating the bone mineral density of the bone first in order to calculate
240 the stopping torque. Gilmer et al describe a dual motor drill that was very accurate in calculating
241 bone mineral density during drilling and the energy of screw insertion, and correlating that to pull-out
242 strength [gilmer2018]. The limitation of their system was the inability to calculate stripping torque
243 and applying it to be used for stopping torque. Two other systems were successful in cortical bone.
244 The mechatronic screwdriver and a “turn-of-the-nut method” of screw tightening, both could sense
245 when the head of the screw makes contact with the bone and detect the rate of change in torque

246 [thomas2008, belkoff2014]. These systems work well in cortical bone, but not well in cancellous
247 bone. Another real time torque system was able to calculate the stripping torque during screw
248 insertion into an ovine vertebral specimen and set a threshold for stopping torque [reynolds2017].
249 The estimate in the system yielded good results from cancellous screws but only in ovine bone, which
250 is not representative of the aged human population as replicated in this study. Orthopaedic surgeons
251 gain experience by training their proprioceptive feedback of torque and axial compressive force as to
252 when to stop tightening a screw. This has been shown to be riddled with human error by the large
253 amount of stripped screws seen in osteopenic bone even with experienced surgeons [andreassen2004,
254 stoesz2014]. This problem is further amplified when one takes into account the learning curve of a
255 trainee surgeon. Torque-limiting screwdrivers have limitations primarily because of the varying
256 degrees of torque required for varying bone mineral densities. A recent systematic review of screw
257 stripping by Fletcher et al highlights the need for development of augmented screwdrivers that are
258 capable of signalling when the ideal non-locking screw tightness occurs in any bone density situation
259 [Fletcher2020]. The results obtained in the current article in testing human bone with different bone
260 densities further advances the legitimacy in developing a device that uses AE monitoring to aid in
261 screw fixation in osteopenic bone. The proposed device has the potential to improve construct
262 stability in the operating room and assist in the developing of trainee orthopedic surgeons. The next
263 stage will be developing an algorithm that enables a device to produce a stop or warning signal for the
264 surgeon to recognize fast enough to halt advancement. As previously described the design and
265 development of a device will need to address sterility and the ergonomics of on-board electronics
266 [pullin2017].

267

268 **5. Conclusion**

269 This experiment succeeded in detecting AE surface waves during screw fixation and stripping through
270 a normal orthopedic screwdriver in human cancellous bone. The AE energy recorded had a positive
271 high correlation to bone mineral density and stripping force. AE energy showed a clear signal during
272 screw purchase through to stripping proving to be a potential technology for the prevention of
273 stripping.

274 **6. Acknowledgements**

275 Lydia Ragan from the Division of Anatomy, Institute of Basic Medical Sciences, University of Oslo,
276 Norway and Department of Physiotherapy, Faculty of Health Sciences, OsloMet - Oslo Metropolitan
277 University, Norway is acknowledged for her help in obtaining and preparing the cadaver bones used
278 for this study. Øystein Horgmo master photographer, Photo- and videodepartment, Institute for
279 Clinical medicine, Oslo University Hospital is acknowledged for taking professional pictures used in

280 the project. Gøril Meland, radiographer, Oslo University Hospital, for her assistance with
281 densitometric measurements.

282 **7. Declaration of conflicting interests**

283 The author(s) declared no potential conflicts of interest with respect to the research, authorship and/or
284 publication of this article.

285 **8. Funding**

286 The authors from Cardiff University were funded by the Medical Research Council as part of a
287 Confidence in Concept scheme. Other author(s) received no financial support for the research,
288 authorship and/or publication of this article.

289 This project was approved by the Norwegian Regional Ethical Committee (REK): 2017/1018/REK
290 sør-øst C

291

292 **9. References**

293 Ab-Lazid R, Perilli E, Ryan MK, Costi JJ, Reynolds KJ. Pullout strength of cancellous screws in
294 human femoral heads depends on applied insertion torque, trabecular bone microarchitecture and areal
295 bone mineral density. *J Mech Behav Biomed Mater*. 2014 Dec;40:354-361. doi:
296 10.1016/j.jmbbm.2014.09.009.

297 Acker WB, Tai BL, Belmont B, Shih AJ, Irwin TA, Holmes JR. Two-Finger Tightness: What Is It?
298 Measuring Torque and Reproducibility in a Simulated Model. *J Orthop Trauma*. 2016 May;30(5):273-
299 7. doi: 10.1097/BOT.0000000000000506.

300 Andreassen GS1, Høiness PR, Skraamm I, Granlund O, Engebretsen L. Use of a synthetic bone void
301 filler to augment screws in osteopenic ankle fracture fixation. *Arch Orthop Trauma Surg*. 2004
302 Apr;124(3):161-5. Epub 2004 Feb 6.

303 Aziz MS, Tsuji MR, Nicayenzi B, Crookshank MC, Bougherara H, Schemitsch EH, Zdero R.
304 Biomechanical measurements of stopping and stripping torques during screw insertion in five types of
305 human and artificial humeri. *Proc Inst Mech Eng H*. 2014 May;228(5):446-455.

306 Belkoff SM, Langdale ER, Knight T. The Johns Hopkins University, assignee. Smart Screw-driver for
307 Preventing Inadvertent Screw Stripping in Bone. US 14/167,144. 2014.

308 Collinge C1, Hartigan B, Lautenschlager EP. Effects of surgical errors on small fragment screw
309 fixation. *J Orthop Trauma*. 2006 Jul;20(6):410-3.

310 Fletcher et al. Surgical performance when inserting non-locking screws: a systematic review. EFORT
311 Open Reviews. 2020 Jan;5(1):26-36. doi.org/10.1302/2058-5241.5.180066

312 Gilmer BB, Lang SD. Dual Motor Drill Continuously Measures Drilling Energy to Calculate Bone
313 Density and Screw Pull-out Force in Real Time. J Am Acad Orthop Surg Glob Res Rev. 2018 Sep
314 25;2(9):e053. doi: 10.5435/JAAOSGlobal-D-18-00053.

315 Gustafson PA, Geeslin AG, Prior DM, Chess JL. Effect of Real-Time Feedback on Screw Placement
316 Into Synthetic Cancellous Bone. Journal of Orthopaedic Trauma. 2016. 30(8), e279–e284.
317 doi:10.1097/bot.0000000000000564.

318 Hinkle,D.E., Wiersma,W., Jurs,S.G.,2003. AppliedStatistics fortheBehavioral Sciences, 5th ed.
319 Houghton Mifflin, Boston.

320 McGuire R, St John K, Agnew S. Analysis of the torque applied to bone screws by trauma surgeons.
321 Comparisons based on years of experience and material of implant construction. Am J Orthopedics
322 (Belle Mead,NJ). 1995;24:254.

323 Pullin R, Wright BJ, Kapur R, McCrory JP, Pearson M, Evans SL, Crivelli D. Feasibility of detecting
324 orthopaedic screw overtightening using acoustic emission. Proc Inst Mech Eng H. 2017
325 Mar;231(3):213-221. doi: 10.1177/0954411916689112.

326 Reynolds KJ, MohtarAA, Cleek TM, Ryan MK, Hearn TC. Automated Bone Screw Tightening to
327 Adaptive Levels of Stripping Torque. Journal of Orthopaedic Trauma. 2017, 31(6), 321–325.
328 doi:10.1097/bot.0000000000000824.

329 Ryan MK, Mohtar AA, Cleek TM, Reynolds KJ. Time-elapsed screw insertion with microCT
330 imaging. Journal of Biomechanics. 2016. 49(2), 295–301. doi:10.1016/j.jbiomech.2015.12.021.

331 Stoesz MJ, Gustafson PA, Patel BV, Jastifer JR, Chess JL. Surgeon perception of cancellous screw
332 fixation. J Orthop Trauma. 2014 Jan;28(1):e1-7. doi: 10.1097/BOT.0b013e31829ef63b.

333 Tankard SE, Mears SC, Marsland D, Langdale ER, Belkoff SM. Does maximum torque mean optimal
334 pullout strength of screws? J Orthop Trauma. 2013 Apr;27(4):232-5. doi:
335 10.1097/BOT.0b013e318279791f.

336 Thomas R, Bouazza-Marouf K, Taylor G. Automated surgical screwdriver: automated screw
337 placement. Proc Inst Mech Eng H. 2008;222: 817–827.

338 Tsuji M, Crookshank M, Olsen M, et al. The biomechanical effect of artificial and human bone
339 density on stopping and stripping torque during screw insertion. J Mech Behav Biomed Mater. 2013
340 June. 22: 146–156.

341 Wickham, H. ggplot2: Elegant Graphics for Data Analysis. Springer-Verlag New York, 2016.

342 Wright B, Ragan L, Niratisairak S, Høiseth A, Strømsøe K, Steen H, Brattgjerd JE. High correlation
343 between mechanical properties and bone mineral parameters in embalmed femurs after long-term
344 storage. *Clin Biomech.* 2018 Nov;59:136-142. doi:10.1016/j.clinbiomech.2018.09